

Anisotropic Ginzburg-Landau theory for arbitrary induction and vortex lattice symmetry: Effects of a - b plane mass anisotropy on the properties of high-temperature superconductors

Archana Achalere* and B. Dey†

Department of Physics, University of Pune, Pune 411 007, India

(Received 2 July 2004; revised manuscript received 29 November 2004; published 14 June 2005)

We study the properties of high-temperature superconductors with a - b plane mass anisotropy. We obtain high precision ideal vortex lattices solutions of the generalized anisotropic nonlinear Ginzburg-Landau equations for arbitrary magnetic induction and vortex lattices symmetry. The effect of a - b plane mass anisotropy on various properties of the high-temperature superconductors, such as, order parameter, magnetic induction, vortex lattice symmetry, reversible magnetization, and shear modulus of the vortex lattice are examined. We compare our results with recent experimental data of $\text{YBa}_2\text{Cu}_4\text{O}_8$.

DOI: 10.1103/PhysRevB.71.224504

PACS number(s): 74.20.De, 74.25.Op, 74.25.Ha

I. INTRODUCTION

Since the discovery of the high-temperature superconductors, interest in studying the vortex configurations in layered superconductors, the most important example being the cuprates high-temperature superconductors, has greatly increased. During the last decade many efforts have been focused on the understanding of the critical properties of type-II superconductors in the frame work of the Ginzburg-Landau theory. Ginzburg-Landau calculations for a single vortex core structure and the geometry of the vortex lattices of layered superconductors have produced many interesting results which have been found to be very important for understanding the field and temperature dependence of the critical-current density in these superconductors.¹

However, most of these studies of Ginzburg-Landau theory are limited to high or low magnetic field where the theory is linear, i.e., the external magnetic fields $B_a \rightarrow B_{c1}$ for isolated vortex solution or $B_a \sim B_{c2}$ for periodic vortex lattice solutions. On the other hand, recent small angle neutron scattering (SANS) and the muon spin rotation (μ SR) experiments of the flux line lattice in high-temperature superconductors² and UPT_3 superconductors³ have shown anomalous magnetic field dependence of the scattering intensities and the vortex lattice structure. Thus, to compare the theoretical results with the SANS and μ SR experiments, study of the nonlinear Ginzburg-Landau equations is required for the entire range of magnetic field $B_{c1} < B_a < B_{c2}$. Some earlier attempts⁴ to study Ginzburg-Landau equations for arbitrary magnetic induction, e.g., the extension of the B_{c2} solutions by Eilenberger, the circular cell method for the extension of B_{c1} (isolated vortex) solutions by Ihle, the variational method by Brandt and also Clem and Hao, had their limitations. While Eilenberger solutions by complex series expansion applies only in a narrow field range below B_{c2} , the circular cell method by Ihle, even though it accurately computes magnetization curves, cannot yield, in principle, properties related to different symmetries of the vortex lattice or to its shear modulus. Similarly, the variational methods accuracy depends on the number of variational parameters used, which have to be compromised with the available computational time and computer efficiency. These restrictions

associated with studying the Ginzburg-Landau equations for arbitrary magnetic induction and any vortex lattice symmetry was overcome by Brandt. In a recent pioneering work, Brandt presented⁵ a novel iteration method that solves Ginzburg-Landau equations for arbitrary magnetic induction and any vortex lattice symmetry with high precision and obtained many results which could not be obtained by earlier methods,⁴ such as the shear modulus of the vortex lattice, etc. This iterative method calculates various properties, such as local magnetic field and order parameter within a few iterative steps for any magnetic induction within the range slightly above the lowest critical field up to upper critical field.

Yet another limitation of the earlier studies of Ginzburg-Landau theory is that most of these studies were for isotropic type-II superconductors. However, it is well known that the high-temperature superconductors are highly anisotropic. Anisotropy can be accounted in terms of an effective mass tensor. For biaxial superconductors m_a , m_b , and m_c are distinct, whereas, for uniaxial superconductors $m_a = m_b$. Even in some cases where the effect of anisotropy were studied, the studies were mostly limited to uniaxial superconductors and for special cases near the lower and upper critical fields B_{c1} and B_{c2} , respectively. Recent experiments have shown that the effect of anisotropy introduces considerable changes, such as distortion of flux line lattice (FLL), vortex lattice melting via an intermediate phase, oblique structure of vortex lattice, etc.⁶ It is observed that many properties of the cuprate high-temperature superconductors are anisotropic mainly due to the nature of the CuO_2 planes. Experiments using small angle neutron scattering as well as scanning tunneling microscopy (STM)⁷ show that there is significant local electronic inhomogeneity which lead to anisotropy even within a CuO_2 plane. For example, $\text{YBa}_2\text{Cu}_3\text{O}_7$ is not in the pure tetragonal phase due to the existence of CuO chains in the b direction.⁸ Large anisotropy between a and b directions for YBCO are seen in the measurements of penetration depth⁹ and the vortex structure by STM.¹⁰ While a tetragonal lattice structure is appropriate for d -wave pairing symmetry, it is now believed that YBCOs have a dominant s -wave component in the order parameter in addition to the d -wave order parameter. This type of two component order parameter is

associated with the orthorhombic symmetry. The orthorhombic lattice symmetry of YBCO originates from the mass anisotropy between the a and b directions, with m_a larger than m_b . Theoretical calculations have shown that the mass anisotropy gives rise to a nonzero s -wave component and clear evidence for this kind of mixing has been found in the recent c -axis Josephson experiments.¹¹ Similarly, measurements of the magnetic-field dependence of the thermal conductivity of BSCCO shows a large anisotropy in the a - b plane¹² suggesting that the number of thermally excited quasiparticles are different along the two axes of the a - b plane.

In order to examine the effect of the mass anisotropy between a and b axis in the CuO_2 plane of various high-temperature superconductors, we present in this paper the results of our high precision numerical study of an anisotropic Ginzburg-Landau theory using Brandt's iteration method.⁵ For better comparison of our theoretical results with the experiments, we study the anisotropic Ginzburg-Landau theory for the entire ranges of magnetic fields $B_{c1} < B_a < B_{c2}$ and arbitrary value of Ginzburg-Landau parameter as well as arbitrary vortex lattice symmetry. To the best of our knowledge, we present for the first time high precision results of the ideal vortex lattice solutions of the nonlinear anisotropic Ginzburg-Landau theory, for arbitrary magnetic induction and vortex lattice symmetry.

We have taken the anisotropy into account based on an anisotropic effective mass approximation within CuO_2 planes and quantified the mass anisotropy through an anisotropic mass parameter $\gamma = m_x/m_y$, where m_x and m_y are the effective masses in the x and y directions, respectively. We assume the vortex lattice to be aligned along the symmetry axes of the crystal and accordingly consider x and y directions parallel to a and b directions of the anisotropic a - b plane, respectively. From the measurement of anisotropy of the penetration depth, the mass anisotropy parameter of $\text{YBa}_2\text{Cu}_3\text{O}_{6.95}$ is obtained as $\gamma = 2.4$.⁹ Of course, the anisotropy of the properties of a superconductor can set in as a result of electron pairing in states with nonzero orbital angular momentum l . We, however, confine ourselves to the simplest s -type pairing (i.e., $l=0$) and therefore regard the effective ψ function of the Ginzburg-Landau theory as a complex scalar. To study the effect of mass anisotropy we consider the generalized anisotropic nonlinear Ginzburg-Landau equations and solve the equations numerically using the high precision iterative method due to Brandt.⁵ The advantages of using Brandt's iterative method are that this genuinely two-dimensional method applies down to very low magnetic inductions $10^{-3} \leq b < 1$, where $b = \bar{B}/B_{c2}$ and also to all relevant Ginzburg-Landau parameters $1/\sqrt{2} \leq \kappa < \infty$. The best advantage of Brandt's method⁵ is that it can yield properties related to the different symmetries of the vortex lattice or its shear modulus. The other methods used for studying the Ginzburg-Landau equations, for example, the circular cell method,⁴ cannot yield properties related to the different symmetries of the vortex lattice or to its shear modulus. Calculation of shear modulus (c_{66}) is very important for determining the stability property of the vortex lattice, such as melting of the vortex lattice. The vortex lattice in the high-temperature superconductors is very soft mainly due to the

large magnetic penetration depth λ_B . It is believed that this softness is further enhanced by layered structure and the mass anisotropy of the high-temperature superconductors. Thermal fluctuations and softening may "melt" the vortex lattice and cause thermally activated depinning of the flux lines. Very recently, the Lindenmann criteria of vortex lattice melting has been formulated in terms of fluctuations of a single vortex over a characteristic length termed as the "single-vortex length" and this length also depends on the shear modulus c_{66} of the vortex lattice.¹³ Therefore, we carefully examine the effect of mass anisotropy on the magnetic field penetration depth [given mainly by the width of the magnetic induction $B(x,y)$ curve] and the shear modulus c_{66} of the vortex lattice.

The paper is organized as follows. Section II describes the theoretical formalism. Section III describes the numerical method used for studying the problem, the results of the numerical calculations, and analysis of the results. Finally, in Sec. IV we conclude with suggestions for future work.

II. THEORETICAL FORMALISM

The free energy of the two-dimensional anisotropic Ginzburg-Landau theory in a geometry such that the applied field is orthogonal to the anisotropic plane can be written in terms of the real gauge invariant functions $\omega(x,y)$ and $\mathbf{Q}(x,y)$ as¹⁴

$$f = \left\langle -\omega + \frac{\omega^2}{2} + (\nabla \times \mathbf{Q})^2 + \frac{\nabla \omega \Gamma \nabla \omega}{4\kappa_y^2 \omega} + \omega \mathbf{Q} \Gamma \mathbf{Q} \right\rangle, \quad (1)$$

where $\mathbf{Q}(x,y) = \mathbf{A}(x,y) - \nabla \phi(x,y)/\kappa_y$ is the supervelocity, \mathbf{A} is the vector potential, $\mathbf{B} = \hat{\mathbf{z}}B = \nabla \times \mathbf{A}$ is the local field, $\omega = |\psi|^2 \leq 1$ is expressed in terms of the Cooper pair density or Ginzburg-Landau ψ function as $\psi(x,y) = \sqrt{\omega(x,y)} \exp[i\phi(x,y)]$, and Γ is the anisotropic mass tensor given by

$$\Gamma = \begin{bmatrix} m_y/m_x & 0 \\ 0 & 1 \end{bmatrix}.$$

Here $\langle \dots \rangle$ denote average value which is obtained by summing over equidistant N points in 2D grid with constant weight $1/N$.⁵ We have introduced here the reduced units¹⁴ $\sqrt{\alpha/\beta}$, $\Phi_0/2\pi\xi_y$, and λ_y for the order parameter $\psi(x,y)$, magnetic vector potential $\mathbf{A}(x,y)$, and all lengths, respectively. The Ginzburg-Landau parameter and the coherence length along the y direction are defined as $\kappa_y = \lambda_y/\xi_y = \Phi_0/2\pi\sqrt{2}B_c\xi_y^2$ and $\xi_y = \hbar/\sqrt{2}m_y\alpha$, respectively, where $B_c^2/8\pi = \alpha/\beta$, α and β being the standard Ginzburg-Landau parameters. Hence the local magnetic field \mathbf{B} is expressed in units of $\sqrt{2}B_c$. We express ω , \mathbf{B} , and $\mathbf{Q}(x,y)$ as the Fourier series

$$\omega(\mathbf{r}) = \sum_{\mathbf{K}} a_{\mathbf{K}} (1 - \cos \mathbf{K} \cdot \mathbf{r}), \quad (2)$$

$$B(\mathbf{r}) = \bar{B} + \sum_{\mathbf{K}} b_{\mathbf{K}} \cos \mathbf{K} \cdot \mathbf{r}, \quad (3)$$

$$\mathbf{Q}(\mathbf{r}) = \mathbf{Q}_A(\mathbf{r}) + \sum_{\mathbf{K}} b_{\mathbf{K}} \frac{\hat{\mathbf{z}} \times \mathbf{K}}{K^2} \sin \mathbf{K} \cdot \mathbf{r}, \quad (4)$$

where the sums are over all reciprocal lattice vector space $\mathbf{K}_{mn} \neq 0$ with $\mathbf{r}=(x,y)$. For vortex positions $\mathbf{R}=\mathbf{R}_{mn}=(mx_1+nx_2,ny_2)$, where m,n are integers, the reciprocal lattice vectors are given by $\mathbf{K}=\mathbf{K}_{mn}=(2\pi/S)(my_2, nx_1+mx_2)$ with $S=x_1y_2=\Phi_0/\bar{B}$ the unit cell area. By varying these lattice symmetry parameters x_1 , x_2 , and y_2 we can continuously go from one particular symmetry of the vortex lattice to the other. For example, for square lattice $y_2=x_1$ and $x_2=0$, while for triangular lattice $y_2=\sqrt{3}x_1/2$ and $x_2=x_1/2$. The shape of the unit cell can be varied periodically from square to triangular if $y_2=x_1$ and by increasing x_2 continuously. This is useful for calculation of shear modulus c_{66} of the vortex lattice as described below. It should be noted that for the mass anisotropic case, the y_2 value of the corresponding triangular vortex lattice need not be equal to $\sqrt{3}x_1/2$ as in the isotropic case. The y_2 value for the anisotropic case can be obtained by calculating the dependence of the free energy $f(x_2=x_1/2, y_2)$ on y_2 and locating the position of the minimum of the free energy. Our goal is to determine the Fourier coefficients $a_{\mathbf{K}}$ and $b_{\mathbf{K}}$ for arbitrary magnetic induction, vortex lattice symmetry, and Ginzburg-Landau parameter. Earlier variational methods of obtaining the approximate solutions of the Ginzburg-Landau equation were limited to considering a finite number of Fourier coefficients $a_{\mathbf{K}}$ and $b_{\mathbf{K}}$ and determining these coefficients by minimizing the corresponding free energy $f(B, \kappa, a_{\mathbf{K}}, b_{\mathbf{K}})$ with respect to these coefficients.⁴ However, the accuracy of the results obtained by these variational methods depended largely on the number of Fourier coefficients used and only few coefficients could be used in practice since the computational time increases very fast with increase in the number of these coefficients. Brandt⁵ recently showed that a much faster and more accurate solutions are obtained by iterating the two Ginzburg-Landau equations $\delta f/\delta\omega=0$ and $\delta f/\delta\mathbf{Q}=0$. For stable and rapidly converging iterations, the trick is to write these two nonlinear Ginzburg-Landau equations as inhomogeneous London-like equations, the inhomogeneous terms coming from the nonlinear terms of the equations. Yet another trick to improve the convergence of the iteration is to add a third equation which minimizes f with respect to the amplitude of ω . The resulting three equations for determining the coefficients $a_{\mathbf{K}}$ and $b_{\mathbf{K}}$ of the required solutions of the anisotropic nonlinear Ginzburg-Landau equations are given by¹⁴

$$a_{\mathbf{K}} := \frac{-4\kappa_y^2 \langle (2\omega - \omega^2 - \omega \mathbf{Q} \Gamma \mathbf{Q} - g) \cos \mathbf{K} \cdot \mathbf{r} \rangle}{\mathbf{K} \Gamma \mathbf{K} + 2\kappa_y^2}, \quad (5)$$

$$a_{\mathbf{K}} := a_{\mathbf{K}} \cdot \frac{\langle (\omega - \omega \mathbf{Q} \Gamma \mathbf{Q} - g) \rangle}{\langle \omega^2 \rangle}, \quad (6)$$

$$b_{\mathbf{K}} := \frac{-2 \langle [\omega B - \bar{\omega}(B - \bar{B}) + p] \cos \mathbf{K} \cdot \mathbf{r} \rangle}{\frac{m_x}{m_y} \mathbf{K} \Gamma \mathbf{K} + \bar{\omega}}, \quad (7)$$

where $g = \nabla \omega \Gamma \nabla \omega / 4\kappa_y^2$ and $p = (\nabla \omega \times \mathbf{Q}) \cdot \hat{\mathbf{z}}$. Here the notation $:=$ denotes replacement.

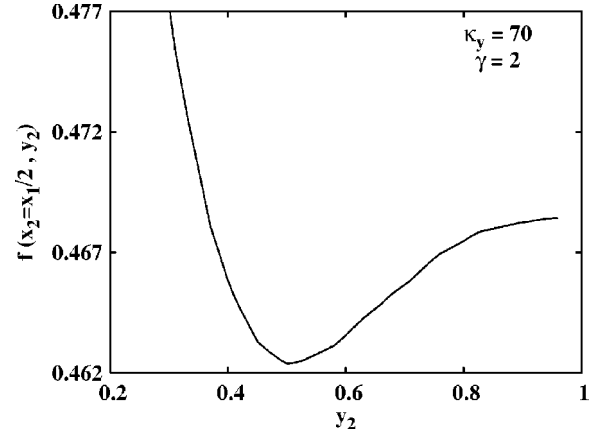


FIG. 1. Free energy in units B_c^2/μ_0 versus y_2 (in units x_1) for $\kappa_y=70$ and mass anisotropy parameter $\gamma=2$.

III. NUMERICAL CALCULATIONS AND RESULTS

To start with, we calculate the dependence of the free energy $f(x_2=x_1/2, y_2)$ on y_2 and find the value of y_2 which minimises the free energy, for various values of the mass anisotropy parameter. We find that for the isotropic case ($\gamma=1$) the free energy is minimized for $y_2=\sqrt{3}x_1/2$, as expected and for the anisotropic case ($\gamma>1$) the corresponding value of y_2 is not equal to $\sqrt{3}x_1/2$ but it depends on the particular value of the mass anisotropy parameter $y_2=y_2(\gamma)$. For example, for $\gamma=2$ case, the free energy $f(x_2=x_1/2, y_2)$ is minimized for $y_2=0.5x_1$. This is shown in Fig. 1, where we have plotted $f(x_2=x_1/2, y_2)$ as a function of y_2 for $\gamma=2$. Similarly, we find that for the mass anisotropy parameter $\gamma=3, 4, 5, 6$, and 7 , the free energy is minimized for $y_2=0.635x_1, y_2=0.71x_1, y_2=0.779x_1, y_2=0.866x_1$, and $y_2=0.92x_1$, respectively.

We iterate the three iteration Eqs. (5)–(7) to determine the coefficients $a_{\mathbf{K}}$ and $b_{\mathbf{K}}$. Following Brandt,⁵ we start the iteration with the coefficients $a_{\mathbf{K}}=a_{\mathbf{K}}^A$ and $b_{\mathbf{K}}=0$, where $a_{\mathbf{K}}^A$ denote the Abrikosov value for the anisotropic system¹⁴ and then follow the order of the iteration sequence as follows: we iterate the first two equations [Eqs. (5) and (6)] a few times to relax ω and then iterate all three equations Eqs. (5)–(7) to relax B . The number of such triple iteration steps required for the solutions to remain constant up to the desired accuracy depend on the parameter values in the theory as well as on the desired symmetry of the vortex lattice. Our numerical results shows that even small variations of the anisotropy parameter $\gamma=m_x/m_y$ have significant effect on several properties of the ideal vortex lattice, such as the order parameter, magnetic induction profile, the reversible magnetization, the shear modulus, etc. To compare our numerical results with the available experimental data, we use parameter values in our calculations appropriate to anisotropic high-temperature superconductors YBCO. For example, the measured κ values for $\text{YBa}_2\text{Cu}_4\text{O}_8$ polycrystals¹⁵ and $\text{Nd}_{1.85}\text{Ce}_{0.15}\text{CuO}_{4-\delta}$ single crystals¹⁶ are $\kappa=70$ and $\kappa=80$, respectively. Similarly, from the measurements of the penetration depth, the mass anisotropy parameter for $\text{YBa}_2\text{Cu}_3\text{O}_{6.95}$ is obtained as $\gamma=2.4$.⁹

The solutions of the anisotropic nonlinear Ginzburg-Landau equations are obtained for arbitrary values of the

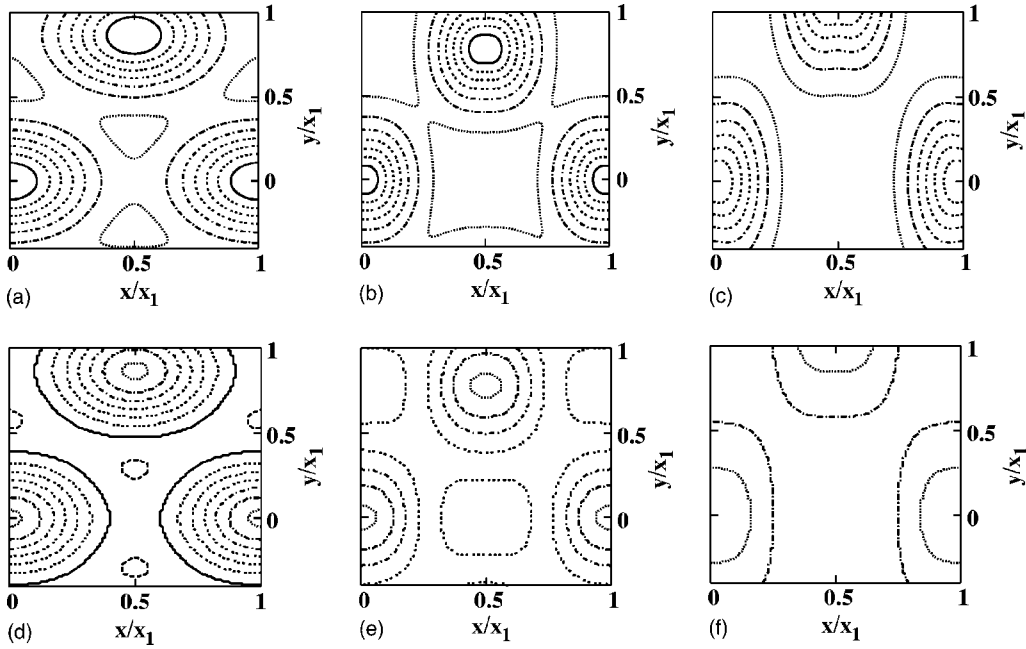


FIG. 2. Contour plots showing vortex lattice of order parameter $\omega(x,y)$ for (a) $\gamma=1$, (b) $\gamma=5$, (c) $\gamma=10$, magnetic induction $B(x,y)$ for (d) $\gamma=1$, (e) $\gamma=5$, (f) $\gamma=10$, and $b=\bar{B}/B_{c2}=0.4$.

various parameters involved, such as mass anisotropy parameter γ , Ginzburg-Landau parameter κ_y , magnetic induction parameter $b=\bar{B}/B_{c2}$ and the vortex lattice symmetry parameters x_2/x_1 and y_2/x_1 . The results are shown in the figures. It is clear from these figures that the a - b plane mass anisotropy have significant effect on the physical properties of the high temperature superconductors.

Figure 2 shows the contour plots of the profiles $\omega(x,y)$ and $B(x,y)$ for different values of the mass anisotropy parameter γ . The effects of the mass anisotropy on the order parameter and the magnetic induction are very much evident from these plots. For a given value of the parameters κ_y and b , the width of the order parameter $\omega(x,y)$ and the magnetic induction $B(x,y)$ decreases with increase of mass anisotropy parameter γ . There is also an associated distortion of the individual vortex profile with increase of mass anisotropy. For a given value of the mass anisotropy parameter γ , the amplitudes as well as the width of the order parameter and magnetic induction profile depends on the magnetic induction parameter b . However, the shape of the curves remains qualitatively same for all values of κ_y . Similar behavior is also observed in the study of the isotropic case.⁵ Figure 3 shows the plot of the peak amplitude variation of $B(x,y)$ profile with mass anisotropy parameter γ . As has been mentioned above, the variation of the amplitude and width of $B(x,y)$ profile is directly related to the shear modulus of the the vortex lattice since the shear modulus depends on the penetration depth of the magnetic field. Figure 4 shows the variation of width of the order parameter profile $\omega(x,0)$ and $B(x,0)$ with magnetic induction parameter b and mass anisotropy parameter γ . Since the shape of the profiles of $\omega(x,y)$ and $B(x,y)$ becomes asymmetric with increase of mass anisotropy parameter γ , we have plotted the width of the profiles along a particular direction in the x - y plane, which we

chose along the x axis. We define the width of the profile as the distance (along the x axis) where the amplitude of the respective profile is half of its peak value. The widths so defined approximately gives the characteristic lengths of the systems, i.e., coherence length and the penetration depth. For a given value of κ_y and magnetic induction parameter b , there is significant decrease in the width of the order parameter profile $\omega(x,0)$ and the magnetic field $B(x,0)$ with increase of mass anisotropy. Similar behavior is also seen for the order parameter profile $\omega(0,y)$ and the magnetic induction $B(0,y)$. The shape of the curves in Fig. 4 remains qualitatively the same for all values of $\kappa_y > 1/\sqrt{2}$.

To examine the dependence of the equilibrium applied magnetic field B_a on the mass anisotropy, we have obtained the reversible magnetization curve $M(B_a)$ of the ideal vortex lattice for the entire range of the applied magnetic fields $B_{c1} < B_a < B_{c2}$, i.e., for arbitrary magnetic induction $0 < b < 1$ and various values of the mass anisotropy parameter γ . The magnetization is defined by the well-known relation

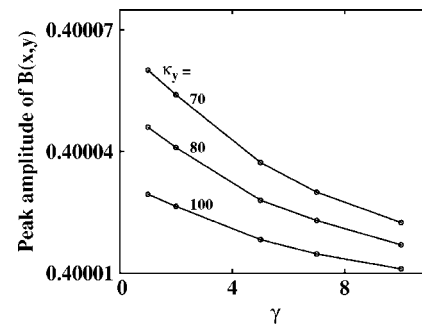


FIG. 3. Variation of peak amplitude of $B(x,y)$ versus mass anisotropy parameter $\gamma=m_x/m_y$ for $\kappa_y=70, 80, 100$.

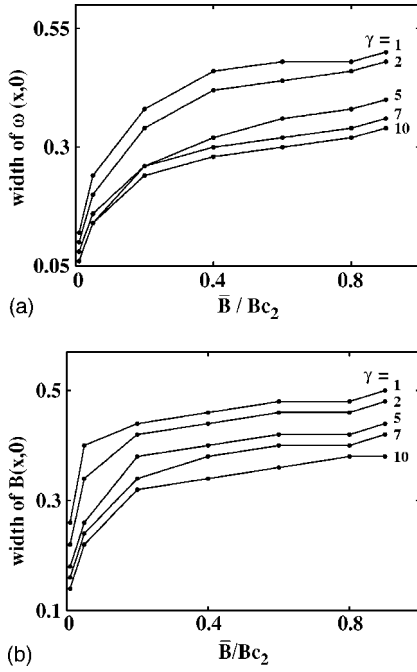


FIG. 4. Plots of width of $\omega(x,0)$ and $B(x,0)$ with $b=\bar{B}/B_{c2}$ for various values of the mass anisotropy parameter $\gamma=1,2,5,7,10$ and $\kappa_y=70$.

$$-4\pi M = B_a - \bar{B}. \quad (8)$$

The equilibrium applied field B_a is obtained numerically from the virial theorem for the vortex lattice

$$B_a = \frac{\langle \omega - \omega^2 + 2B^2 \rangle}{\langle 2B \rangle} \quad (9)$$

which is proven in Ref. 17. Figure 5 compares our numerically obtained result with that of the experimentally observed behavior¹⁵ of the reversible magnetization curve of the vortex lattice for $\text{YBa}_2\text{Cu}_4\text{O}_8$. The open circles are the experimental results and the continuous line is the numerical result obtained for the parameter values $\kappa=70$ and $\gamma=2$ which are approximately equal to the measured parameter values of YBCO. The agreement between the experimental and nu-

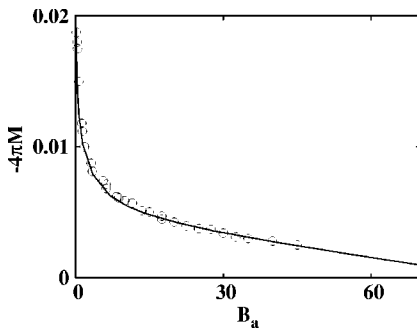


FIG. 5. Reversible magnetization curve calculated for $\kappa_y=70$ and mass anisotropy parameter $\gamma=2$. The solid line represent numerically calculated results and the circles gives the experimental data for $\text{YBa}_2\text{Cu}_4\text{O}_8$ (Ref. 15).

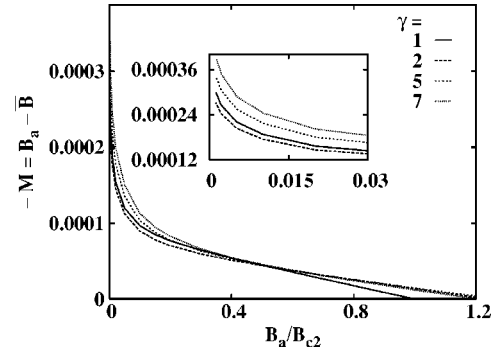


FIG. 6. Reversible magnetization curves (in units B_{c2}) for various values of the mass anisotropy parameter $\gamma=1,2,5,7$ and $\kappa_y=70$.

merical plot is excellent. Figure 6 shows the variation of the reversible magnetization with mass anisotropy parameter γ . It can be seen that the variations are appreciable for low values of equilibrium applied magnetic field B_a . For lower values of B_a , the reversible magnetization for mass anisotropic case ($\gamma=2$) is lower than that of its value for isotropic case ($\gamma=1$), but the corresponding values increases for higher values of the mass anisotropy. However, for higher values of the equilibrium magnetic field ($B_a/B_{c2} > 0.5$), the reversible magnetization for the mass anisotropic case is always larger than that of its value for the symmetric case. For mass anisotropic case, one can notice that there is a very small (but nonzero $\sim 10^{-5}$) value of the reversible magnetization at $B_a/B_{c2}=1$ which goes to zero at $B_a/B_{c2}=1.2$. This may be an indication of recent observation that mass anisotropy enhances upper critical field B_{c2} value.¹⁸

We now compute the shear modulus of the vortex lattice. As has been mentioned above, the advantage of using the Brandt's iteration method is that it allowed us to calculate the effect of mass anisotropy on the shear modulus c_{66} of the vortex lattice for arbitrary values of the magnetic induction parameter b and Ginzburg-Landau parameter κ_y . For the isotropic case, the shear modulus can be expressed by the difference of the free energies of the rectangular lattice f_{rect} (with $x_2=0$ and $y_2=\sqrt{3}x_1/2$) and the triangular lattice f_{tr} (with $x_2=x_1/2$ and $y_2=\sqrt{3}x_1/2$).⁵ This is so since the free energy for constant unit cell height y_2 varies practically sinusoidally with x_2 , i.e., $f(x_2) \approx f_{\text{tr}} + [1 + \cos(2\pi x_2/x_1)](f_{\text{rect}} - f_{\text{tr}})/2$. We have checked the validity of this relation even for mass anisotropic case. For each value of the mass anisotropy parameter considered here, we have checked that the free energy for the corresponding constant unit cell height $y_2(\gamma)$ varies practically sinusoidally with x_2 . The shear modulus for the mass anisotropic systems thus depends on three parameters $c_{66}=c_{66}(b, \kappa, \gamma)$ and is given by

$$c_{66} = 2\pi^2 [y_2(\gamma)/x_1]^2 \times \{f_{\text{rect}}[x_2=0, y_2(\gamma)] - f_{\text{tr}}[x_2=x_1/2, y_2(\gamma)]\}. \quad (10)$$

For $\gamma=1$ [$y_2(\gamma)=\sqrt{3}x_1/2$] this reduces to the same expression of c_{66} for the isotropic system.⁵ We have studied the behavior of the shear modulus with change of mass anisotropy param-

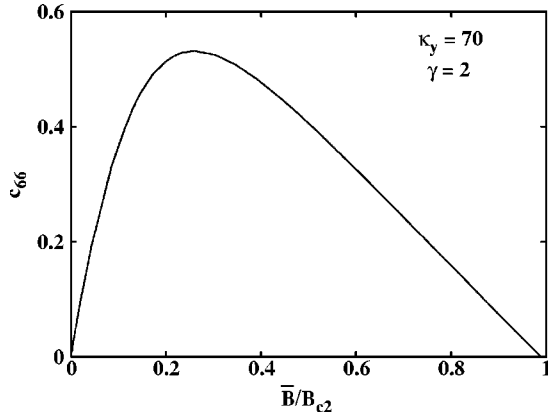


FIG. 7. The shear modulus c_{66} in units B_c^2/μ_0 versus b for $\kappa_y = 70$ and mass anisotropy parameter $\gamma = 2$.

eter γ . The plot of c_{66} versus the magnetic induction parameter b for a particular value of the mass anisotropy parameter $\gamma = 2$ is shown in Fig. 7. The positive value of c_{66} implies that the vortex lattice with the particular symmetry considered (in this case, triangular) is stable. The profile shows that the c_{66} value increases from its zero value with increase of magnetic induction parameter b , reaching a peak value at an intermediate value of b , and then decreases with increase of b to zero value. The profile of the c_{66} plot for the anisotropic case ($\gamma = 2$) looks qualitatively similar to that of the isotropic case ($\gamma = 1$),⁵ however, the peak position (the value of parameter b for which the c_{66} attains peak value) and the peak amplitude of c_{66} changes with increasing mass anisotropy. The peak position and the peak amplitude of c_{66} are important quantities. While the peak amplitude determines the hardness of the vortex lattice (stability of the vortex lattice), the peak position (b value) denotes the magnetic induction at the peak value. Our study of the effect of mass anisotropy on shear modulus shows interesting results. It is observed that the peak value of the amplitude of c_{66} increases with increase of mass anisotropy parameter. For $\gamma = 1$, the peak amplitude value is 0.041 which is in agreement with the value for the symmetric case.⁵ In Fig. 8 we have plotted the peak amplitude value of c_{66} versus mass anisotropy parameters for $\kappa_y = 70$. This is an important result, for it shows that the shear

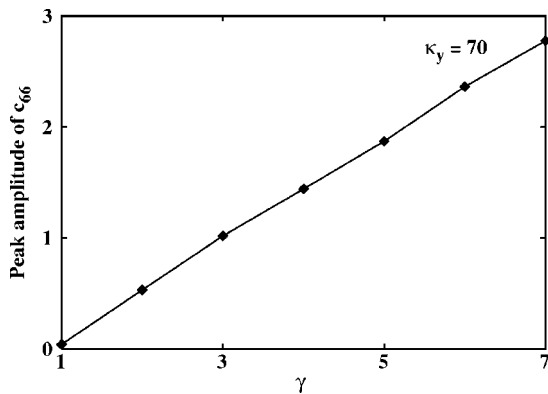


FIG. 8. Peak amplitude of the shear modulus c_{66} (in units B_c^2/μ_0) versus the mass anisotropy parameter γ for $\kappa_y = 70$.

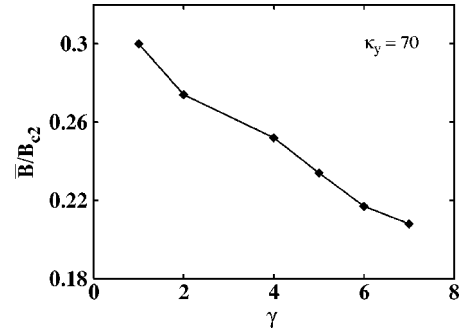


FIG. 9. Peak position of c_{66} versus the mass anisotropy parameter γ for $\kappa_y = 70$.

modulus increases with increase of mass anisotropy or the vortex lattice becomes harder with increase of mass anisotropy. This implies that the ‘melting’ of the vortex lattice with increasing mass anisotropy becomes more difficult. This is contrary to the popular belief that the softening of the vortex lattice is enhanced further by the pronounced anisotropy. This is also expected from our earlier result of the decrease of the penetration depth of the magnetic induction with increasing mass anisotropy parameter as shown in Fig. 4 above. Since the shear modulus $c_{66} \sim 1/\lambda_B^2$, therefore it increases with decrease of the penetration depth and the vortex lattice becomes harder. Similarly, from our numerical calculations we also observe that the value of the magnetic induction at which the amplitude of the c_{66} attains peak value also decreases with increase of the mass anisotropy parameter γ . This is shown in Fig. 9. This implies that for a given value of the Ginzburg-Landau parameter κ_y and at lower magnetic induction, the vortex lattice become harder with increase of mass anisotropy.

IV. CONCLUSIONS

In conclusion, we have presented a detailed analysis of the generalized anisotropic nonlinear Ginzburg-Landau theory for high-temperature superconductors with a - b plane mass anisotropy. The anisotropic nonlinear Ginzburg-Landau equations are solved using a recently proposed high precision iterative method. We find that it is important to consider the effect of a - b plane mass anisotropy as even a small variations of the mass anisotropy parameter have significant effect on several properties of the anisotropic high-temperature superconductors. Since recent SANS and μ SR experiments in high-temperature superconductors have shown anomalous magnetic field dependence of the scattering intensities and the vortex lattice structure, therefore we have studied the problem for arbitrary magnetic induction instead of restricting near the upper or lower critical fields. We obtain excellent agreement between our numerical results and experimental data of YBCO. Special attention is paid to the role of mass anisotropy on the shear modulus of the vortex lattice and we have obtained the important results that the shear modulus increases with increase of a - b plane mass anisotropy and also that the shear modulus attains its peak value at lower values of magnetic induction with increase of mass

anisotropy. This has very important implication in the melting of the corresponding vortex lattices.

As has been mentioned above, the orthorhombic lattice symmetry of YBCO is related to the mass anisotropy in the a - b plane. Similarly, YBCO have a dominant s -wave component in the order parameter in addition to the d -wave order parameter. This type of two component order parameter is also associated with the orthorhombic symmetry. Therefore, one should further generalize our study of the effect of a - b plane mass anisotropy on properties of high-temperature superconductors by considering Ginzburg-Landau theory for two component order parameter. There have been some attempts in this direction, such as the two-component Ginzburg-Landau theory to determine the structure of the vortex lattice of heavy fermion superconductor UPT₃ (Ref. 19) and other superconductors with odd-parity superconducting order parameter, e.g., Sr₂RuO₄,²⁰ and also for supercon-

ductors with $d_{x^2-y^2}$ symmetry with an induced s -wave component.²¹ However, these studies are restricted to isotropic case and also for magnetic field near lower (B_{c1}) and upper (B_{c2}) critical fields. As discussed above, it is required to further generalize these two-component Ginzburg-Landau theories by taking into account the effect of mass anisotropy and study the problem for arbitrary magnetic induction and vortex lattice symmetry for better comparison of the theoretical results with experimental observations. Work along this direction is in progress and will be reported elsewhere.

ACKNOWLEDGMENTS

The authors would like to thank Dr. E. H. Brandt for help with the numerics. The authors would also like to thank DAE (India) for financial assistance through the BARC-Pune University research collaboration program.

*Electronic address: archana@physics.unipune.ernet.in

†Electronic address: bdey@physics.unipune.ernet.in

- ¹For reviews, see E. H. Brandt, Rep. Prog. Phys. **58**, 1465 (1995); G. Blatter, M. V. Feigel'man, V. B. Geshkenbein, A. I. Larkin, and V. M. Vinokur, Rev. Mod. Phys. **66**, 1125 (1994).
- ²B. Keimer, W. Y. Shih, R. W. Erwin, J. W. Lynn, F. Dogan, and I. A. Aksay, Phys. Rev. Lett. **73**, 3459 (1994); J. Appl. Phys. **76**, 6778 (1994); J. E. Sonier, R. F. Kiefl, J. H. Brewer, D. A. Bonn, J. F. Carolan, K. H. Chow, P. Dosanjh, W. N. Hardy, R. Liang, W. A. MacFarlane, P. Mendels, G. D. Morris, T. M. Riseman, and J. W. Schneider, Phys. Rev. Lett. **72**, 744 (1994).
- ³C. Broholm, G. Aeppli, R. N. Kleiman, D. R. Harshman, D. J. Bishop, E. Bucher, D. Li. Williams, E. J. Ansaldo, and R. H. Heffner, Phys. Rev. Lett. **65**, 2062 (1990); A. Huxley, R. Cubitt, D. McPaul, E. Forgan, M. Nutley, H. Mook, M. Yethiraj, P. Lejay, D. Caplan and J. M. Pnison, Physica B **223–224**, 169 (1996); U. Yaron, P. L. Gammel, G. S. Boebinger, G. Aeppli, P. Schiffer, E. Bucher, D. J. Bishop, C. Broholm, and K. Mortensen, Phys. Rev. Lett. **78**, 3185 (1997); N. H. van Dijk, A. de Visser, J. J. M. Franse, and L. Taillefer, J. Low Temp. Phys. **93**, 101 (1993); R. A. Fisher, S. Kim, B. F. Woodfield, N. E. Phillips, L. Taillefer, K. Hasselbach, J. Flouquet, A. L. Giorgi, and J. L. Smith, Phys. Rev. Lett. **62**, 1411 (1989); G. Bruls, D. Weber, B. Wolf, P. Thalmeier, B. Lthi, A. d. Visser, and A. Menovsky, *ibid.* **65**, 2294 (1990).
- ⁴G. Eilenberger, Z. Phys. **180**, 32 (1964); D. Ihle, Phys. Status Solidi B **47**, 423 (1971); **47**, 429 (1971); Z. Hao, J. R. Clem, M. W. McElfresh, L. Civale, A. P. Malozemoff, and F. Holtzberg, Phys. Rev. B **43**, 2844 (1991), E. H. Brandt, Phys. Status Solidi B **51**, 354 (1972); W. V. Pogosov, K. Kugel, A. Rakhmanov, and E. Brandt, Phys. Rev. B **64**, 064517 (2001).
- ⁵E. H. Brandt, Phys. Rev. Lett. **78**, 2208 (1997).
- ⁶P. G. Kealey, D. Charalambous, E. M. Forgan, S. L. Lee, S. T. Johnson, P. Schleger, R. Cubitt, D. McK. Paul, C. M. Aegerter, S. Tajima, and A. Rykov, Phys. Rev. B **64**, 174501 (2001); E. W. Carlson, A. H. Castro Neto, and D. K. Campbell, Phys. Rev. Lett. **90**, 087001 (2003).
- ⁷B. Lake, H. M. Rnnow, N. B. Christensen, G. Aeppli, K. Lefmann, D. F. McMorrow, P. Vorderwisch, P. Smeibidl, N. Mangkorntong, T. Sasagawa, M. Nohara, H. Takagi, and T. E. Mason, Nature (London) **415**, 299 (2002); B. Lake, G. Aeppli, K. N. Clausen, D. F. McMorrow, K. Lefmann, N. E. Hussey, N. Mangkorntong, M. Nohara, H. Takagi, T. E. Mason, and A. Schrder, Science **291**, 1759 (2001); J. E. Hoffman, E. W. Hudson, K. M. Lang, V. Madhavan, H. Eisaki, S. Uchida, and J. C. Davis, *ibid.* **295**, 466 (2002).
- ⁸W. A. Atkinson and J. P. Carbotte, Phys. Rev. B **52**, 10 601 (1995).
- ⁹K. Zhang, D. A. Bonn, S. Kamal, R. Liang, D. J. Baar, W. N. Hardy, D. Basov, and T. Timusk, Phys. Rev. Lett. **73**, 2484 (1994).
- ¹⁰I. Maggio-Aprile, Ch. Renner, A. Erb, E. Walker, and Ø. Fischer, Phys. Rev. Lett. **75**, 2754 (1995).
- ¹¹W. Belzig, C. Bruder, and M. Sigrist, Phys. Rev. Lett. **80**, 4285 (1998); K. A. Kouznetsov, A. G. Sun, B. Chen, A. S. Katz, S. R. Bahcall, J. Clarke, R. C. Dynes, D. A. Gajewski, S. H. Han, M. B. Maple, J. Giapintzakis, J.-T. Kim, and D. M. Ginsberg, *ibid.* **79**, 3050 (1997).
- ¹²Y. Ando, J. Takeya, Yasushi Abe, X. F. Sun, and A. N. Lavrov, Phys. Rev. Lett. **88**, 147004 (2002).
- ¹³Jan Kierfeld and V. Vinokur, Phys. Rev. B **69**, 024501 (2004).
- ¹⁴I. G. de Oliveira, M. M. Doria, and E. H. Brandt, Physica C **341–348**, 1069 (2000).
- ¹⁵J. Sok, M. Xu, W. Chen, B. J. Suh, J. Gohng, D. K. Finnemore, M. J. Kramer, L. A. Schwartzkopf, and B. Dabrowski, Phys. Rev. B **51**, 6035 (1995).
- ¹⁶A. Nugroho, I. M. Sutjahja, A. Rusydi, M. O. Tjia, A. A. Menovsky, F. R. de Boer, and J. J. M. Franse, Phys. Rev. B **60**, 15 384 (1999).
- ¹⁷M. M. Doria, J. E. Gubernatis, and D. Rainer, Phys. Rev. B **39**, 9573 (1989).
- ¹⁸Wonkee Kim, Jian-Xin Zhu, and C. S. Ting, Phys. Rev. B **61**, 4200 (2000).
- ¹⁹R. Joynt, Phys. Rev. Lett. **78**, 3189 (1997); R. Joynt and L. Taillefer, Rev. Mod. Phys. **74**, 235 (2002).
- ²⁰A. P. Mackenzo and Y. Maeno, Rev. Mod. Phys. **75**, 657 (2003).
- ²¹Y. Ren, Ji-Hai Xu, and C. S. Ting, Phys. Rev. Lett. **74**, 3680 (1995).